Role of Molecular Structure on X-ray Diffraction in Uniaxial and Biaxial Phases of Thermotropic Liquid Crystals[†]

Bharat R. Acharya,*[,‡] Shin-Woong Kang,[§] Veena Prasad,[||] and Satyendra Kumar[§]

Platypus Technologies, 5520 Nobel Drive, Madison, Wisconsin 53705, Department of Physics, Kent State University, Kent, Ohio 44240, and Center for Liquid Crystal Research, Jalahalii, Bangalore-560013, India

Received: November 24, 2008; Revised Manuscript Received: January 20, 2009

X-ray diffraction is one of the most definitive methods to determine the structure of condensed matter phases, and it has been applied to unequivocally infer the structures of conventional calamitic and lyotropic liquid crystals. With the advent of bent-core and tetrapodic mesogens and the discovery of the biaxial nematic phase in them, the experimental results require more careful interpretation and analysis. Here, we present *ab-initio* calculations of X-ray diffraction patterns in the isotropic, uniaxial nematic, and biaxial nematic phases of bent-core mesogens. A simple Meier-Saupe-like molecular distribution function is employed to describe both aligned and unaligned mesophases. The distribution function is decomposed into two, polar and azimuthal, distribution functions to calculate the effect of the evolution of uniaxial and biaxial nematic orientational order. The calculations provide satisfactory semiquantitative interpretations of experimental results. The calculations presented here should provide a pathway to more refined and quantitative analysis of X-ray diffraction data from the biaxial nematic phase.

I. Introduction

In the liquid phase of matter, intermolecular positional order correlations do not extend beyond the nearest neighbor, and it possesses the highest symmetry, that is, the system is invariant under any (translational, rotational, or other) symmetry operations. The crystalline phase, on the other hand, possesses long-range bond orientational and positional orders and, therefore, has lower symmetry. Lattices corresponding to crystalline solids are invariant only under specific symmetry operations corresponding to the space group of the crystal.[1] Some materials with nonspherical building blocks (e.g., rods, discs, parallelepiped, bent rods) exhibit a number of intermediate phases between the crystalline solid and isotropic liquid. The systems in these phases are collectively known as liquid crystals. Liquid crystals (LCs) possess long-range orientational order[2] and short- or long-range bond-orientational or positional orders along different spatial directions. These unique characteristics of liquid crystals make them particularly attractive systems to experimentally validate some of the fundamental theoretical concepts of physics (e.g., phase transitions, scaling laws, symmetry breaking, 2D melting, etc.). Their exquisite sensitivity to external stimuli such as electrical, mechanical, and magnetic fields and changes in the chemical and biological environment forms the basis of their numerous technological applications, such as liquid crystal displays, photonics, and biochemical sensors.

On the basis of the structure and the nature of interaction between molecules, a variety of LC phases have been predicted and observed.[2] The simplest LC phase is the nematic (N) phase in which the long axes of cylindrically symmetric molecules are, on average, aligned along a common direction, known as the director ($\vec{n}$). The N phase does not possess any translational order. On the basis of symmetry considerations, Frieser[3] predicted two types of uniaxial and one biaxial nematic phases. The uniaxial nematic (N_u) phase possesses a unique director ($\vec{n}$) and is invariant under rotation about the director, that is, it has $C_{2\infty}$ symmetry. Existence of the nematic phase requires anisotropic interactions between molecules to affect orientational order among them. This is generally achieved by designing molecules with a rigid core (for anisotropic interaction) and flexible end groups to render interactions weak. On the basis of these criteria, a number of LCs with uniaxial symmetry have been designed and synthesized and are widely used in commercial applications.

The biaxial nematic (N_b) phase, on the other hand, has two distinct directors, the primary director ($\vec{n}$) and a secondary director ($\vec{m}$) orthogonal to $\vec{n}$. The N_b phase possesses C_{2h} or C_{2v} symmetry and therefore has lower symmetry than the N_u phase. Until recently, only the complex tertiary lyotropic (micellar) systems were known to exhibit the N_b phase.[4] Although the lyotropic systems validated the theoretical prediction of the existence of the N_b phase, they could not be quantitatively explored for technological applications because of the small anisotropy in physical properties such as birefringence and dielectric anisotropy related to the biaxial order. Therefore, the search for the N_b phase in thermotropic LC materials continued for several decades. Synthesis of several molecules with different architectures including anisotropic but flat, fork-shaped, mixtures of rod and discs, parallelepiped, and bent-core molecules was attempted.[5] However, several of the initial claims of the biaxial phase, based on optical microscopy,[6] were later not confirmed[7] by X-ray and NMR experiments.

X-ray diffraction (XRD) has been used as a nondestructive tool to identify phases,[2] study phase transitions,[8−11] and extract the structural information of solids and liquids.[12] The atomic planes in a solid crystal reflect X-rays and give rise to Bragg peaks corresponding to the interplaner distance. In the liquid phase, since the positional order correlations are limited only to the nearest neighbors, the X-ray structure factor can be approximated by Fourier transform of the pair correlation

[†] Part of the "PGG (Pierre-Gilles de Gennes) Memorial Issue".
* To whom correspondence should be addressed.
[‡] Platypus Technologies.
[§] Kent State University.
[||] Center for Liquid Crystal Research.

10.1021/jp810333r CCC: $40.75
Published on Web 03/19/2009

function. Therefore, X-ray diffraction consists of a diffuse ring in the reciprocal space.[13] For anisotropic (e.g., rod-like) molecules, there are two lengths associated with the nearest-neighbor correlations. Therefore, two liquid-like diffused rings corresponding to the two lengths are observed. The diffused ring at the small/large angle corresponds to the effective length/diameter of the molecules. The diffraction pattern from a multidomain (i.e., unaligned) N_u phase is similar to that of an isotropic liquid as the measured X-ray scattering pattern from randomly oriented domains in an unaligned sample is statistically averaged over all director orientations. For a monodomain N_u phase, the diffraction pattern reflects the symmetry of the phase. Consequently, the two diffuse rings condense into two quasi Bragg peaks, one at small angle along $\vec{n}$ and the second peak in the transverse direction (for details, see ref 2). The intensity distribution in the outer reflections of the aligned N_u phase has been exploited to extract the distribution function and the order parameter of the nematic phases of rod-shaped mesogens[14] and virus[15] systems.

Over the past three decades, molecules of various architectures have been synthesized with the goal of obtaining the N_b phase in low molecular weight thermotropic materials. The focus has been on molecules with inherent molecular biaxiality. A liquid crystalline phase in systems that combine features of rods and discs was reported to exhibit two brush disclinations, which was thought to be a hallmark of the N_b phase.[16] The XRD pattern from this system exhibited two additional diffuse peaks along the direction orthogonal to the director. The existence of the additional peaks was originally thought to be an indication of N_b phase. However, these additional peaks only confirmed the molecular biaxiality. In order to confirm the phase biaxiality, one needed to probe molecular order in two directions perpendicular to $\vec{n}$.

The discovery of bent-core mesogens[18] put the possibility of the biaxial nematic phase at the forefront of the field of LCs. Most of the bent-core materials did not exhibit a nematic phase. However, rigid bent-core mesogens comprised of the oxadiazole derivative formed the nematic phase that was studied with XRD in the presence of an applied electric field. We used the form factor and the structure factor to calculate the scattering intensity from an aligned monodomain nematic phase. The calculated X-ray intensity distribution is quite distinct in the two transverse planes containing the nematic director. Combined with experimental results, this analysis led to the discovery of the theoretically predicted but highly elusive biaxial nematic phase in a low molar mass bent-core thermotropic LC.[19,20] This discovery was later confirmed by NMR,[21] Raman scattering,[22] and electro-optical[23] experiments and atomistic simulations.[24]

In this paper, we calculate the evolution of the four diffuse X-ray peaks for bent-core molecules. Maier−Saupe-type single-parameter distribution functions were used to describe the orientation of the long molecular axis and the planes of the bent-core molecules. These results, when combined with the results of X-ray diffraction, demonstrate that the bent-core molecules can exhibit both uniaxial and biaxial nematic phases and reveal the nature of the phase between them. This paper is organized as follows. We describe X-ray diffraction first from the (isotropic) spherical molecules and then from the isotropic and nematic phase of (anisotropic) rod-like molecules. Next, we consider the bent-core molecule and calculate the diffraction intensity in its isotropic and nematic phases. We introduce the molecular distribution functions and vary the degree of the "order" parallel and transverse to the primary nematic director. The calculated diffracted intensity profiles are then compared with recent results from XRD experiments on these compounds, where both directors are aligned under the influence of a treated surface and, then, one of them is reoriented with an applied electric field. Finally, the two possible routes to the biaxial nematic phase from the isotropic phase are discussed.

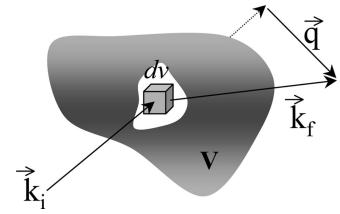

Figure 1. Schematic diagram depicting the X-ray diffraction from a sample.

II. X-ray Diffraction

When X-ray radiation with initial wave vector $\vec{k}_i$ is scattered from volume V with electron density $\rho(\vec{r})$, the wave vector changes to $\vec{k}_f$ with momentum transfer $\vec{q} = \vec{k}_i - \vec{k}_f$ (see Figure 1). The complex function describing the amplitude and the phase of the scattered wave is given by the Fourier transform of the electron density as

$$f(\vec{q}) = \int_V \rho(\vec{r})\exp(\vec{q}\cdot\vec{r})\mathrm{d}\vec{r}$$

The scattered intensity in $\vec{q}$-space is given by $I(\vec{q}) = f(\vec{q}) \times f^*(\vec{q})$, where $f^*(\vec{q})$ is the complex conjugate of $f(\vec{q})$. The scattering intensity from a molecule is given by summing over all of the atoms on the molecule

$$I(\vec{q}) = \sum_j f_j(\vec{q})\exp(\mathrm{i}\vec{r}_j\cdot\vec{q})\sum_k f_k(\vec{q})\exp(-\mathrm{i}\vec{r}_k\cdot\vec{q}) = \sum_j\sum_k f_j(\vec{q})f_k(\vec{q})\exp[\mathrm{i}(\vec{r}_j - \vec{r}_k)\cdot\vec{q}]$$

For a system of N molecules, the total scattered intensity at a point in the $\vec{q}$-space is given by averaging over all molecules and their orientations

$$I(\vec{q}) = \left\langle \sum_j\sum_k f_j(\vec{q})f_k(\vec{q})\exp[\mathrm{i}(\vec{r}_j - \vec{r}_k)\cdot\vec{q}]\right\rangle$$

$$I(\vec{q}) = N\langle|f(\vec{q})|^2\rangle + \left\langle \sum_{j\neq k} f_j(\vec{q})f_k(\vec{q})\exp[\mathrm{i}(\vec{r}_j - \vec{r}_k)\cdot\vec{q}]\right\rangle$$

In general, the scattered intensity is expressed as a product of two terms, the form factor $F(\vec{q})$ that depends only on the single particle distribution function and the structure factor $S(\vec{q})$ that includes both spatial and orientational correlations

$$I(\vec{q}) = NF(\vec{q}) \times S(\vec{q})$$

The form factor $F(\vec{q})$ is given by $F(\vec{q}) = \langle|f(\vec{q})|^2\rangle$. The structure factor depends on the relative positions and orientation of two neighboring anisotropic molecules, and is given by[9]

$$S(\vec{q}) = 1 + \frac{1}{NF(\vec{q})}\left\langle \sum_{j\neq k} f_j(\vec{q})f_k(\vec{q})\exp[\mathrm{i}(\vec{r}_j - \vec{r}_k)\cdot\vec{q}]\right\rangle$$

This formulation allows decoupling of the contribution from the form factor and the structure factor under certain conditions. For example, for rod-like molecules in the nematic and isotropic phases, where spatial correlations are small, the scattered intensity at a large angle is approximated by assuming $S(\vec{q}) = 1$.[14] In the smectic-A phase, where the spatial correlations are well-developed, the X-ray scattering is described by assuming

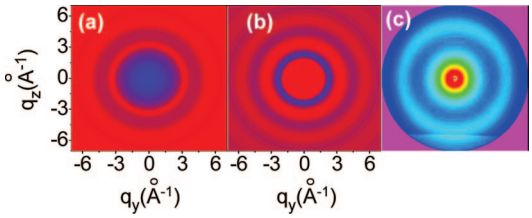

Figure 2. The calculated (a) form factor and (b) scattered intensity from a system of spherical molecules in the q_y-q_z plane. Because of the symmetry of the system, the diffraction pattern in the q_x-q_z plane is identical. (c) The experimentally observed two-dimensional diffraction pattern from a water sample in a capillary tube at room temperature.

that $F(\vec{q}) = 1$.[9] The observed X-ray scattering intensity is then the product $F(\vec{q}) \times S(\vec{q})$ convoluted with the instrumental resolution function. For simplicity, we assume an instrumental resolution function to be infinitely narrow. In that case, the observed intensity in $\vec{q}$-space is given by $I(\vec{q}) = F(\vec{q}) \times S(\vec{q})$.

A. Spherical Molecules. For particles with spherical symmetry, the electronic density is independent of the orientations of the particles, i.e. $f_j(\vec{q}) = f_k(\vec{q})$, and the form factor and the structure factor decouple. For a spatially homogeneous and rotationally invariant fluid of spherical particles of radius R, with uniform density ρ, the form factor is given by[25]

$$f(\vec{q}) = \rho\frac{3[\sin(qR) - qR\cos(qR)]}{(qR)^3}$$

The expression for the structure factor reduces to $S(\vec{q}) = 1 + (1/N)\langle\sum_{j\neq k}\exp[i(\vec{r}_j - \vec{r}_k)\cdot\vec{q})\rangle$, and it depends on the nature of interaction between the particles. For hard-sphere potential, the structure factor is given by[26]

$$S(\vec{q}) = S(q) = \frac{1}{1 + 24\eta G(2Rq)/(2Rq)}$$

where,

$$G(A) = \frac{\alpha}{A^2}(\sin A - A\cos A)/A^2 + \frac{\beta}{A^3}[2A\sin A + (2 - A^2)\cos A - 2] + \frac{\gamma}{A^5}[-A^4\cos A + 4\{(3A^2 - 6)\cos A + (A^3 - 6A)\sin A + 6\}]$$

and $\alpha = (1 + 2\eta)^2/(1 - 2\eta)^4$, $\beta = -6\eta(1 + \eta/2)^2/(1 - 2\eta)^4$, $\gamma = \eta\alpha/2$, and η is the packing fraction. For a system of spherical particles with random packing, $\eta = 0.638$.

Figure 2 shows the form factor (panel a) and diffracted intensity (panel b) for spherical molecules of 2.75 Å diameter in the q_y-q_z plane. As expected for the randomly distributed closed-packed system of hard spheres, the form factor, structure factor, and the scattered intensity all exhibit spherical symmetry. Since the system is rotationally invariant, the diffraction patterns in the q_x-q_z plane are identical. Figure 2c shows experimental diffraction pattern of water filled in a capillary that was exposed to synchrotron X-ray radiation of $\lambda = 0.765$ Å. The pattern was recorded using an area detector. As calculated, the XRD pattern shows a diffuse ring corresponding to the diameter of the water molecule.

B. Rod-Shaped Molecules. When spherical symmetry is broken by the molecule's shape anisotropy, the effect of the reduced symmetry needs to be included in both the form factor and the structure factor. For anisotropic (e.g., rod- or disk-like) molecules, $f_j(\vec{q}) \neq f_k(\vec{q})$, and the structure and form factors do not decouple except when all of the molecules are aligned parallel to each other. In general, the XRD data is analyzed by approximating the scattered intensity either by the form factor $F(\vec{q})$ alone in the high-$\vec{q}$ limit or with an approximate form of the structure factor $S(\vec{q})$ in the low-$\vec{q}$ regime.

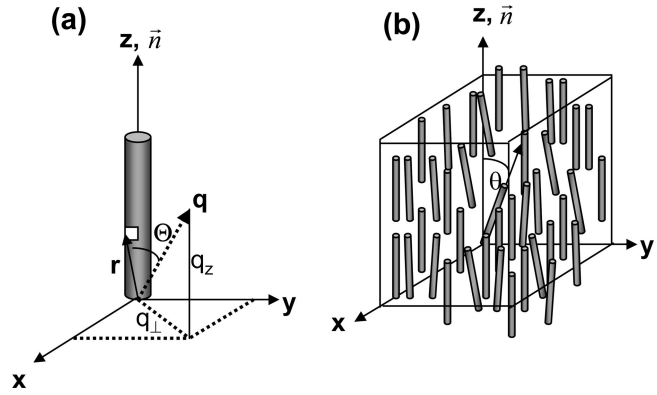

Figure 3. (a) Schematic diagram depicting the orientation of the scattering vector and the rod-like LC molecule in the laboratory frame of reference. (b) The rod-like molecules, on average, align parallel to the director $\vec{n}$. The quality of alignment along $\vec{n}$ is determined by the distribution function $f(\theta)$.

For a system of rod-like molecules with uniform electron density distribution, the expression for the form factor can be evaluated analytically using a cylindrical coordinate system as shown in Figure 3a. For a molecule of length L and radius R, oriented at angle θ with respect to the nematic director, the complex function $f(\vec{q}')$ is given by[27]

$$f(\vec{q}') = \rho\frac{[\exp(iq'_zL) - 1]}{2iq'_zL} \times \frac{J_1[q'_\perp R]}{q'_\perp R}$$

where, $J_1(x)$ is a Bessel's function of the first kind of argument x. The wave vectors $\vec{q}$ in the laboratory coordinate system and $\vec{q}'$ in the molecular coordinate system are related to each other through the transformations

$$\begin{aligned} q'_x &= q_x \\ q'_y &= q_y\cos\theta + q_z\sin\theta \\ q'_z &= -q_y\sin\theta + q_z\cos\theta \end{aligned}$$

In the nematic phase, the distribution of rod-like molecules along the director $\vec{n}$ can be approximated by a Maier-Saupe-like distribution function,[15] $f(\theta) = N_\gamma\exp[\gamma\cos^2\theta]$, where N_γ is the normalization constant such that

$$\int_0^{\pi/2}\sin\theta d\theta f(\theta) = 1$$

and γ is a parameter that depends on the strength of intermolecular interactions leading to the alignment of molecules. Small γ [i.e., $f(\theta) \sim 1$] means random alignment of molecules, and therefore, the isotropic phase. A large value of γ [i.e., $f(\theta) \sim \delta(\theta)$] means preferred alignment of molecules along the director and thus a well-aligned nematic phase. In the following calculations, we use $\gamma = 0.01$ (instead of 0, to avoid any singularity in calculations) to represent the isotropic phase and $\gamma = 5$ for the nematic phase. The form factor is then given by

$$F(\vec{q}) = \int_0^{\pi/2}|f(\vec{q})|^2 f(\theta)\sin\theta d\theta$$

The form factor $F(\vec{q})$ depends on the distribution of molecules about the director determined by the distribution function. When molecules are randomly aligned, the form factors in q_x-q_z and q_y-q_z planes are identical, that is, $F(\vec{q})$ is spherically symmetric. On the other hand, when the molecules show preferential

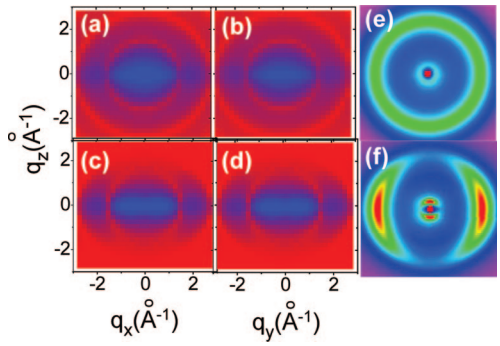

Figure 4. Distribution of the X-ray scattering intensity for rod-like molecules in two orthogonal planes in $\vec{q}$-space. Panels (a) and (b) correspond to $\gamma = 0.01$, and panels (c) and (d) correspond to $\gamma = 5$ in the q_x-q_z and q_y-q_z planes, respectively. The 2-d X-ray diffraction pattern from the (e) isotropic and (f) nematic phases of 4-cyano-4′-pentylbiphenyl.

alignment along $\vec{n}$, the form factor shows a strongly anisotropic azimuthal distribution.[27] The development of orientational order has a significant effect on the form factor at both small and large $\vec{q}$ values. More importantly, the form factor remains identical in the two orthogonal planes.

Since the form and structure factors are coupled, it is difficult to obtain an analytical expression for the structure factor. However, for a distribution of rod-like molecules with their long molecular axes aligned along the z-direction, the structure factor for small $\vec{q}$ can be approximated by a Lorentzian. It has been modified to have three different positional order correlation lengths,[11] comparable to the molecular dimensions, in the three spatial dimensions as

$$S(\vec{q}) \propto \frac{1}{1 + \xi_z^2(q_z - q_0)^2 + \xi_x^2 q_x^2 + \xi_y^2 q_y^2}$$

where, the ξ_i's are the correlation lengths along the respective directions and $q_0 = 2\pi/d$ is the smectic wave vector (d = smectic periodicity). For simplicity, the correlation lengths can be approximated as $\xi_x = \xi_y = 2R$ and $\xi_z = L$. It should be noted that at small $\vec{q}$, the structure factor assumes a modulation along the director, that is, the z-direction, with correlation length comparable to the nearest-neighbor distance L. The observed X-ray scattering intensity is then the product $F(\vec{q}) \times S(\vec{q})$ averaged over different orientations of domains in the nematic phase convoluted by the instrumental resolution function. Although in the real experimental situation the scattered intensity also depends on the mosaic (domain) distribution,[10] for simplicity, we assume that the system consists of a single domain and that the instrumental resolution function is infinitely narrow. In that case, the observed intensity in the $\vec{q}$-space is given by $I(\vec{q}) = F(\vec{q}) \times S(\vec{q})$.

Using the above approximations, we have calculated $I(\vec{q})$ in two orthogonal planes for the isotropic and nematic phases of the rod-like molecules (Figure 4). Evidently, the scattering intensity shows azimuthally symmetric diffuse peaks (Figure 4a, upper left panel), which are identical in the two orthogonal planes, at large angles in the isotropic phase ($\gamma = 0.01$). Since we used a static structure factor with fixed correlation lengths that gives two quasi-Bragg peaks at $q_z = q_0$, there are two diffuse peaks at small q values even for the isotropic phase instead of diffuse rings.

In the nematic phase ($\gamma = 5$), the scattered intensity at large $\vec{q}$ becomes anisotropic and strongly concentrated near the x-y plane. At small $\vec{q}$, the intensity is concentrated on the z-axis in the two diffuse peaks at $q_z = \pm q_0$ along the director. The outer reflections are located perpendicular to the nematic director at the values of q_x and q_y corresponding to the diameter of the rods. It should be noted that the diffraction patterns are symmetric with respect to the z-axis and almost identical in the two (q_z-q_x) and (q_z-q_y) planes in this uniaxial nematic phase. Calculated diffraction profiles are in qualitative agreement with the experimental results obtained for the isotropic and nematic phases of 4-cyano-4′-pentylbiphenyl (Figure 4, right panels). This material exhibits a uniaxial nematic phase below the isotropic phase. These diffraction patterns were obtained with the sample in a capillary tube that was heated to the isotropic phase and then cooled in the presence of an *in-situ* magnetic field of 2.5 kG. Synchrotron X-ray radiation with a 0.765 Å wavelength and a two-dimensional image plate detector (MAR3450) were used.

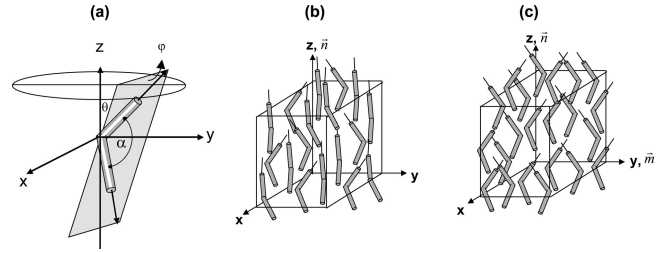

Figure 5. (a) Orientation of a bent-core molecule with apex angle α in the laboratory frame of reference. Two segments of the molecules are a aligned along z-direction of their respective coordinate systems. The distributions of the molecular long axis and the plane of the bent-core molecules about the primary director $\vec{n}$ and secondary director $\vec{m}$ are given by the distribution functions $f(\theta)$ and $f(\varphi)$, respectively. Organization of the bent-core molecules is shown in the (b) uniaxial and (c) biaxial nematic phases.

C. Bent-Core Molecules. Let us now reduce the symmetry further by introducing a bend at the center of the cylindrical rod-like molecules. Since such a bent-core molecule has two segments joined at an apex, a plane containing the two segments can be defined as the segment plane. We approximate the structure of these molecules by two solid cylindrical segments of length L and radius R connected at a fixed apex angle α (refer to Figure 5a). While calculating the form factor for such bent-core molecules, one must take into account, both, the alignment of their long axes and the orientation of the segment planes (or their apex). The form factor for the bent-core molecule in the laboratory frame of reference can be calculated by treating each segment in its own frame of reference with the constraint that the angle between the two segments be fixed at α. The form factor is then given by

$$f(\vec{q}) = f_{\text{seg1}}(\vec{q'}) + f_{\text{seg2}}(\vec{q''})$$

where, $\vec{q'}$ and $\vec{q''}$ are the wave vectors in their respective frame of reference and can be related to $\vec{q}$ through the proper coordinate transformations.[27] Clearly, the form factor depends not only on the angle between the two segments but also on the relative orientation of the segment planes. For simplicity, we assume that the segment plane is always perpendicular to the x-y plane in the laboratory frame. We allow the molecular long axis and the segment plane to have a finite distribution about the z- and y-axes, respectively.

In the biaxial nematic phase, molecules are aligned, on average, along the primary director $\vec{n}$, and the planes of the molecules are aligned along secondary director $\vec{m}$; distribution of the molecules can be specified by two angles, θ and φ. We

introduce an orientational distribution function $f(\theta,\varphi)$, with the normalization condition

$$\int_0^{2\pi} d\varphi \int_0^{\pi/2} \sin\theta d\theta f(\theta,\varphi) = 1$$

which describes the orientational distribution of the long axes and segment planes. The form factor can be written as,

$$F(\vec{q}) = \int_0^{2\pi} d\varphi \int_0^{\pi/2} |f(\vec{q})|^2 f(\theta,\varphi) \sin\theta d\theta$$

The effect of the form factor on the scattered intensity depends not only on the electron density distribution of individual molecule but also on the molecular orientational distribution. The actual distribution of molecular planes depends on the interactions between the molecules, dimensions of the molecule, and temperature. For simplicity, we assume that the molecular distribution function can be decomposed into two independent functions, $f(\theta,\varphi) = f(\theta) \times f(\varphi)$. Both distribution functions are approximated by Maier-Saupe-like functions, $f(\theta) = N_\gamma \exp[\gamma \cos^2 \theta]$ and $f(\varphi) = N_\beta \exp[\beta \cos^2 \varphi]$, where $N_{\gamma,\beta}$ are the normalization constants, and γ and β reflect strengths of the interactions. In the isotropic phase with $\gamma = \beta = 0$, both the long axes and segment planes are randomly distributed. A phase with $\gamma > 0$ and $\beta = 0$, where the long axes are oriented along $\vec{n}$ and segment planes are randomly distributed, is the uniaxial nematic phase (Figure 5b). The phase with $\gamma > 0$ and $\beta > 0$ gives rise to orientational order of both the long axes and the segment planes along $\vec{n}$ and $\vec{m}$, respectively. This corresponds to the biaxial nematic phase (Figure 5c).

Using these approximations, the form factor for a system of bent-core molecules has been calculated in two orthogonal planes for different values of γ and β. For a system with $\gamma = 5$ and $\beta = 0.01$ (i.e., for the uniaxial phase), the form factor shows identical behavior in the two orthogonal planes at both small and large q values. However, when the azimuthal symmetry is broken, and the segment planes align along $\vec{m}$, the form factor becomes different in the two orthogonal planes. Although the patterns in two orthogonal planes appear to be identical for large $\vec{q}$, they are very different at small $\vec{q}$. The XRD pattern at small $\vec{q}$ displays the symmetry of the bent-core molecules.[27]

The structure factor for bent-core molecules, as for the rod-like system, is related to the short-range mass density fluctuations. At small $\vec{q}$, the mathematical (Lorentzian) expression used for rod-like systems can be modified as

$$S(\vec{q}) \propto \frac{1}{1 + \xi_z^2(q_z - q_0)^2 + \xi_x^2 q_x^2 + \xi_y^2 q_y^2}$$

Here, q_0 is the smectic wave vector. In contrast to the calamitic system where the two correlation lengths perpendicular to the director are identical, the effective positional correlation lengths, the ξ_i's for the bent-core molecules along three orthogonal directions are now different. Assuming that molecules are aligned along the director $\vec{n}$ (z-axis), the system possesses liquid-like short-range correlations in this direction. The correlation lengths along the two orthogonal directions perpendicular to $\vec{n}$ depend on the relative orientation of segment planes. If the segment planes exhibit preferential alignment along the y-axis (Figure 5c), the two transverse correlation lengths become different but reflect the effective molecular dimensions in the respective directions. For simplicity, correlation lengths can be approximated as

$$\xi_y = 2L \sin\left(\frac{\pi - \alpha}{2}\right)$$

$$\xi_x = 2R$$

and

$$\xi_z = 2L \cos\left(\frac{\pi - \alpha}{2}\right)$$

The observed X-ray scattering intensity is the product $F(\vec{q}) \times S(\vec{q})$ averaged over different orientations in the nematic phase. Note that, beyond imposing nematic order and shape biaxiality, that is, asymmetry in the correlation lengths along x- and y-directions, no explicit assumption regarding the phase biaxiality has been made. In order to simplify things further, we assume a monodomain sample. Then, $I(\vec{q}) = F(\vec{q}) \times S(\vec{q})$.

For a system of bent-core molecules, $I(\vec{q})$ depends on the orientational distributions determined by parameters β and γ. Figure 6 shows plots of the intensity $I(\vec{q})$ in the q_x-q_z plane calculated for molecules with $L = 27$ Å, $R = 2.5$ Å, and $\alpha = 140°$ for different values of β and γ. In the isotropic phase ($\beta = 0.01$, $\gamma = 0.01$), $I(\vec{q})$ at large $\vec{q}$ is azimuthally isotropic (Figure 6a). Since we have used a static structure factor, two diffuse peaks appear instead of one diffused ring at small $\vec{q}$. On the other hand, for a nematic phase where both the long molecular axes and the segment planes are well aligned ($\gamma = 5$ and $\beta = 5$), the azimuthal symmetry of the diffraction pattern at the large angle is broken, and two diffuse crescents are observed in two orthogonal planes (Figure 6b). Figures 6c and 6d show diffraction patterns from bent-core molecule A110 [3-{[4-(4-dodecyloxybenzoiloxy)benzylidene]amino}-2-methylbenzoic acid 4-(dodecylphenylazo)phenyl ester] that exhibits a nematic phase at 178.0 °C and an isotropic phase at 183.0 °C. As calculated, the diffraction patterns in the isotropic and nematic phases consist of one diffused ring (Figure 6c) and two diffuse peaks (Figure 6d), respectively, at large angles.

The nature of interactions among the bent-core molecules dictates the characteristics of the nematic phase below the isotropic phase. The system may first enter the uniaxial nematic phase with identical diffraction patterns in the two orthogonal directions. The diffraction patterns reflect the symmetry of the

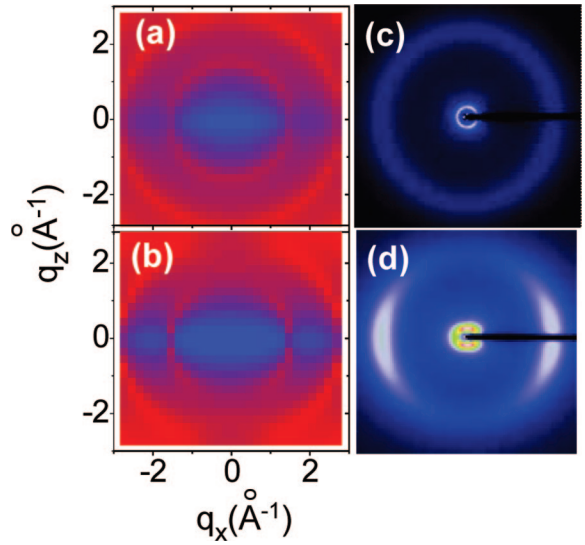

Figure 6. (a) Calculated distribution of the scattered intensity $I(\vec{q})$ in q-space for (a) randomly distributed ($\gamma = \beta = 0.01$) and (b) almost perfectly oriented ($\gamma = \beta = 5$) bent-core molecules. The experimentally observed scattered intensity distributed in (c) isotropic and (d) nematic phases of bent-core molecules.

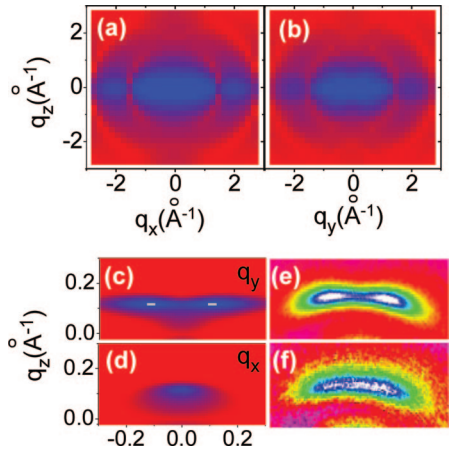

Figure 7. Variation of the scattered intensity $I(\vec{q})$ on two orthogonal planes in q-space for near-perfect alignment of bent-core molecules ($\gamma = \beta = 5$) in (a) q_x-q_z and (b) q_y-q_z planes. Panels (c) and (d) depict the corresponding enlarged views of the diffraction patterns at a small angle. The panels on the right show the observed scattered intensity from a bent-core liquid crystal supported between two beryllium substrates (e) without and (f) with a square-wave voltage of amplitude 5 V applied between them.

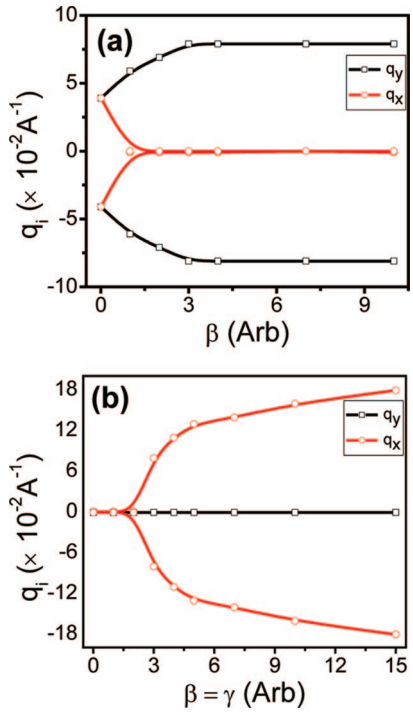

Figure 8. (a) Dependence of the position of the intensity maxima in two orthogonal planes, in q-space, on β for a system of bent-core molecules where the molecules prefer alignment of the long molecular axes prior to the alignment of segment planes. For these calculations,$\gamma = 3$ was used to describe the distribution of the long molecular axes along the primary director. (b) Evolution of the intensity maxima in two orthogonal planes as a function of $\gamma = \beta$ for a system where the molecular interaction prefers simultaneous alignment of the long molecular axes and segment planes.

molecules and consist of four diffuse peaks at small $\vec{q}$ instead of the two as for rod-like molecules. At large angles, the XRD pattern of this uniaxial nematic phase consists of two diffuse peaks corresponding to the transverse separation between the molecules.

As the molecular order evolves, the segment planes start to align parallel to the secondary director $\vec{m}$, resulting in the biaxial nematic phase. The diffraction patterns at large angles do not change significantly. However, at small angles, the diffraction patterns depend on the relative orientation of $\vec{q}$ and the segment planes. When the X-ray beam is incident perpendicularly to the segment planes, the diffraction pattern consists of four diffuse peaks. However, when the X-ray beam is incident parallel to the segment plane, only two peaks are observed. Figures 7a and 7b depict the calculated diffraction patterns for nearly perfect alignment along both $\vec{n}$ and $\vec{m}$ ($\gamma = 5$ and $\beta = 5$). Figures 7c and 7d show a magnified view of the diffraction patterns.

In order to perform the XRD experiment in these two orthogonal orientations, a film of A110 was sandwiched between two polished beryllium substrates coated with unidirectionally rubbed polyimide films. The cells were assembled with antiparallel rubbing directions, having a ~20 μm gap, and filled with the LC in the isotropic phase. The cell was slowly cooled to the nematic phase, to 166.8 °C, and placed in the path of X-ray beam to record XRD patterns. A low-strength square-wave ac electric field (of 5 V amplitude) was applied across the two beryllium plates to reorient $\vec{m}$ while keeping $\vec{n}$ aligned along the rubbing direction. Figures 7e and 7f depict the upper half of the small-angle XRD pattern without and with the electric field, respectively. In the absence of an external field, the segment planes orient perpendicular to the X-ray beam, and the XRD pattern shows four diffuse peaks (Figure 7e). In the presence of an external field, the second director becomes perpendicular to the plates, rendering the X-ray beam parallel to the segment planes. Now, the XRD exhibits two diffuse peaks (Figure 7f). The existence of two distinct diffraction patterns (two diffuse peaks in one plane and four diffuse peaks in the other) in two orthogonal orientations is the unambiguous evidence for the biaxiality of the phase.

It should be noted that the coupling strength between the applied electric field and the dielectric anisotropy of individual molecules is insufficient to overcome (thermal) director fluctuations and have any significant influence on the nematic order. It has previously been shown that in order to have any influence on the director fluctuations and induce a uniaxial order, one would need enormous fields (magnetic field $B \sim 300$ Tesla[28] or an electric field $E \sim 3 \times 10^7$ V/m[29]). The value of E is comparable to the dielectric breakdown field of LC materials[31] and is at least 2 orders of magnitude greater than the electric field (2.5×10^5 V/m) applied in these experiments. Therefore, the possibility of a field-induced biaxial order can be completely ruled out.

The X-ray diffraction pattern from the uniaxial nematic phase of bent-core molecules has four diffuse peaks in both of the orthogonal planes. Here, we note that the mere existence of four diffuse peaks is not an indicator of the phase biaxiality. The four peaks merely reflect the symmetry of the molecules. A fully developed and aligned biaxial nematic phase will have four/two diffuse peaks with the X-ray beam incident perpendicular/parallel to the segment plane, respectively. When the system enters the biaxial nematic phase from the uniaxial nematic phase and $\vec{m}$ is well aligned, the four diffuse peaks in one of the planes will remain unchanged, and the four diffuse peaks in the other direction will gradually merge into two.

Let us now consider the case when a nematic phase grows from the isotropic phase such that the long axes and the segment planes gradually align along respective directions $\vec{n}$ and $\vec{m}$. At a temperature close to the transition, both the uniaxial and biaxial order parameters are small. As a consequence, there are two identical pairs of diffuse peaks in two orthogonal directions. The system effectively appears as a uniaxial phase of a rod-like system. At lower temperatures, both uniaxial and biaxial

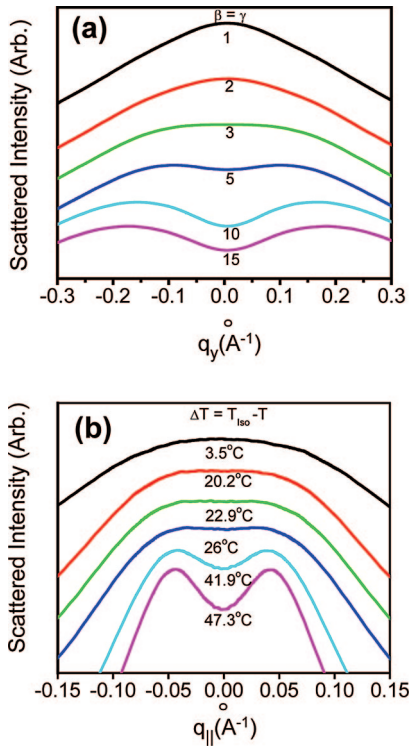

Figure 9. (a) Variation of the calculated integrated intensity as a function of q_y for different values of $\beta = \gamma$. (b) Variation of the integrated intensity as a function of the wave vector for azo-substituted bent-core liquid crystals for different reduced temperatures ΔT. We note that the sample was in a capillary tube with an external magnetic field and that no attempt was made to align the secondary director.

nematic order parameters gradually grow. At a sufficiently low temperature, the diffraction patterns obtained with X-ray beam perpendicular to the segment planes splits into four diffused peaks. However, the two diffuse peaks in the transverse direction remain qualitatively unchanged. Appearance of distinct diffraction patterns in two orthogonal planes is an indication of the biaxial nematic phase.

Figure 8a depicts the scattered intensity maxima in two orthogonal planes for a well-developed uniaxial nematic phase ($\gamma = 3$) as a function of increasing orientational order of the segment planes, that is, the evolution of the biaxial nematic phase from a uniaxial nematic phase. It is clear that the four diffuse peaks in the plane perpendicular to the segments will remain the same, but the peaks in the orthogonal plane gradually will merge into two in a well-aligned biaxial nematic phase. Figure 8b shows the case where the molecular interactions favor simultaneous growth of the two orientational orders. For this system, the diffraction ring observed with the X-ray beam perpendicular to the $\vec{m}$-$\vec{n}$ plane gradually transforms into four diffuse peaks. In the orthogonal direction, they condense into two diffuse peaks.

Figure 9a shows the evolution of the azimuthally integrated intensity of the diffraction pattern in the q_z-q_y plane as a function of β ($= \gamma$). Clearly, the two diffuse peaks split into four peaks as the segment planes become orientationally ordered. In order to realize these predictions in an experiment, we used recently synthesized azo-substituted bent-core liquid crystals.[31] The LC material was filled in a thin capillary tube and placed in the path of X-rays of 0.7653 Å wavelength. The sample was then heated to the isotropic phase and then slowly cooled to nematic phase in the presence of *in-situ* 2.5 kG magnetic field. Figure 9b shows the integrated intensity as a function of momentum transfer for various values of reduced temperature. The qualitative agreement between the calculated and the measured diffraction patterns suggests that both the molecular axes and the segment planes simultaneously align along the respective directions. Near the nematic-isotropic transition, the uniaxial orientational order along $\vec{n}$ is much higher than the orientational order for the segment planes along $\vec{m}$, and therefore, the system behaves as uniaxial nematic. As the nematic phase develops at lower temperatures, the degree of order of segment planes becomes significant, and the system becomes biaxial.

We note that the expression for the scattered intensity with the modified form factor can be used to fit the experimental data and to extract the fitting parameters. These parameters, in turn, can be used to deduce the distribution functions. Since the order parameter can be expressed in terms of the distribution functions,[27] the extracted distribution function can then be employed to calculate the uniaxial and biaxial order parameters. However, it does not seem intuitive to write an analytical expression for the scattered intensity for these complicated structures. The scattered intensity, therefore, will involve a straightforward two-dimensional numerical integration.

III. Summary

We have shown that the observed X-ray diffraction from an ensemble of molecules depends strongly on molecular structure. In order to extract the information about the molecular organization, the effect of the form factor needs to be taken into account. Inclusion of the molecular form factor in the analysis becomes more important when the molecules possess shape biaxiality. By introducing distribution functions to describe orientations of the long molecular axes and planes of the bent-core molecules, we have demonstrated that the X-ray diffraction pattern from the system of bent-core molecules in the two orthogonal directions perpendicular to the primary director $\vec{n}$ can be used to identify the uniaxial and biaxial nematic phases. Qualitative agreement between the calculate and experimental diffraction patterns suggests that measurements of the scattered X-ray intensity in the two orthogonal planes can be used to estimate the biaxial order parameters and to study the uniaxial−biaxial phase transition.

Acknowledgment. This work was supported, in part, by the National Science Foundation Grant DMR-0806991. Use of the Advanced Photon Source (APS) was supported by the U.S. Department of Energy, Basic Energy Sciences, Office of Science, under Contract No. W-31-109-Eng-38. The Midwest Universities Collaborative Access Team (MUCAT) sector at the APS is supported by the U.S. Department of Energy, Basic Energy Sciences, Office of Science, through the Ames Laboratory under Contract No. W-7405-Eng-82.

References and Notes

(1) Kittel, C. *Introduction to Solid State Physics*, 8th ed.; John Wiley & Sons: New York, 2005.
(2) Kumar S., Ed. *Liquid Crystals: Experimental Study of Physical Properties and Phase Transitions*; Cambridge University Press: New York, 2001.
(3) Freiser, M. J. *Phys. Rev. Lett.* **1970**, *24*, 1041.
(4) Yu, L. J.; Saupe, A. *Phys. Rev. Lett.* **1980**, *45*, 1000.
(5) Bruce, D. W. *Chem. Rec.* **2004**, *4*, 10.
(6) (a) Chandrasekhar, S.; Raja, V. N.; Sadashiva, B. K. *Mol.Cryst. Liq.Cryst. Lett.* **1990**, *7*, 65. (b) Malthele, J.; et al. *C.R. Acad. Sci. Paris* **1986**, *303*, 1073.
(7) (a) Shenouda, I. G.; Shi, Y.; Neubert, M. *Mol. Cryst. Liq. Cryst.* **1994**, *257*, 209. (b) Hughes, J.; et al. *Chem. Phys.* **1997**, *107*, 9252.
(8) Als-Nielsen, J.; Birgeneau, R. J.; Kaplan, M.; Litster, J. D.; Safinya, C. R. *Phys. Rev. Lett.* **1977**, *39*, 352.

(9) McMillan, W. L. *Phys. Rev. A* **1972**, *6*, 936.
(10) Primak, A.; Fisch, M.; Kumar, S. *Phys. Rev. Lett.* **2002**, *88*, 035701.
(11) McMillan, W. L. *Phys. Rev.* **1973**, *A 8*, 328.
(12) de Gennes, P. G. *The Physics of Liquid Crystals*; Oxford University Press: Cambridge, U.K., 1974.
(13) Chaikin, P. M.; Lubensky, T. C. *Principles of Condensed Matter Physics*; Cambridge University Press: Cambridge, U.K.
(14) Leadbetter, A. J.; Norris, E. K. *Mol. Phys.* **1979**, *38*, 669.
(15) Purdy, K.; Dogic, Z.; Fraden, S.; Lurio, L.; Mochrie, S. G. J. *Phys. Rev. E* **2003**, *67*, 031708.
(16) Chandrasekhar, S.; Nair, G. G.; Praefcke, K.; Singer, D. *Mol. Cryst. Liq. Cryst.* **1996**, *288*, 7.
(17) Kouwer, P. H. J.; Mehl, G. H. *J. Am. Chem. Soc.* **2003**, *125*, 1117.
(18) (a) Link, D. R. *Science* **1998**, *88*, 2181. (b) Noiri, T.; et al. *J. Mater. Chem.* **1996**, *6*, 1231. (c) Lubensky, T. C.; Radzihovsky, L. *Phys. Rev. E* **2002**, *66*, 031704.
(19) Acharya, B. R.; Primak, A.; Dingemans, T. J.; Samulski, E. T.; Kumar, S. *Pramana* **2003**, *61*, 231.
(20) Acharya, B. R.; Primak, A.; Kumar, S. *Phys. Rev. Lett.* **2004**, *92*, 145506.
(21) Madsen, L. A.; Dingemans, T. J.; Nakata, M.; Samulski, E. T. *Phys. Rev. Lett.* **2004**, *92*, 145505.
(22) Southern, C. D.; Brimicombe, P. D.; Siemianowski, S. D.; Jaradat, S.; Roberts, N.; Gortz, V.; Goodby, J. W.; Gleeson, H. F. *Europhys. Lett* **2008**, *82*, 56001.
(23) Yu, J.; et al. *Korean J. Phys.* **2008**, *52*, 342.
(24) Palaez, J.; Wilson, M. R. *Phys. Rev. Lett.* **2006**, *97*, 267801.
(25) Rayleigh, L. *Proc. R. Soc. London, Ser. A* **1911**, *84*, 25–38.
(26) Pederson, J. S. *Adv. Colloid Interface Sci.* **1997**, *70*, 171.
(27) Acharya, B. R.; Kang, S.-W.; Kumar, S. *Liq. Cryst.* **2008**, *35*, 109.
(28) Mukhopadhyay, R.; Yethiraj, A.; Bechhoefer, J. *Phys. Rev. Lett.* **1999**, *83*, 4796.
(29) Lelidis, I.; Nobili, M.; Durand, G. *Phys. Rev. E* **1999**, *48*, 3818.
(30) Dirking, I. *J. Phys. D: Appl. Phys.* **2001**, *34*, 806.
(31) Prasad, V.; et al. *J. Am. Chem. Soc.* **2005**, *127*, 17224–9.

JP810333R